Analysis of Object Taken from Patient John Smith

Report Author: Steve Colbern

25 January, 2009

Background Information

Personal History of Subject

Mr. John Smith is in his 40's, and is married with 3 children. The subject has a strong technical background, and is currently a researcher in the Materials Science field.

Case History

The subject has had a lifelong history of UFO sightings, and missing time experiences. On the night of February 28, 2008, Mr. Smith was alone in his house. About 10:30 PM, he sighted two unusually large raccoons in the avocado tree, in his back yard. He fed the animals, and observed for them for some time. Mr. Smith then went to bed, and slept until approximately 8:00 AM the following morning.

Upon awakening, Mr. Smith noticed a burning pain in the tip of his left, second toe, and a soreness on the right side of his head. Inspection revealed two apparent puncture wounds on the underside of the end of the left, second, toe, and a scratch on its right side. One of the puncture wounds in the toe was found to fluoresce green under ultraviolet (UV) illumination.

Over the next four days, the pain in the toe increased, and felt like a strong electric shock, whenever any weight was placed on the end of the affected toe. The pain was at a maximum four days after the incident, and decreased slowly thereafter. Mr. Smith then saw Dr. Roger Leir, who obtained X-rays of Mr. Smith's left foot. A small (~3 mm) foreign object showed up on the X-rays, under the end of the distal phalanx bone of the left, second, toe.

The object resembled a bent piece of wire on the X-ray. Dr. Leir commented that the object had approximately the same X-ray density as human bone. A subsequent CAT scan of the left foot confirmed the presence of a foreign object in the same toe.

Gaussmeter, and radio frequency analyzer (RF) tests were done on the object, on August 21, 2008, by Dr. Leir, at his Thousand Oaks office, while it was still in Mr. Smith's body. These tests indicated that the object was emitting radio waves in the Gigahertz, Megahertz, and Extremely Low Frequency (ELF) bands. The object also generated a magnetic field of > 10 mGauss.

The object in Mr. Smith's toe was removed surgically on September 6, 2008, by Dr. Roger Leir, and Dr. John Matriciano. The object was apparently brittle, and broke into 12 pieces during removal.

Pathology tests on the tissue surrounding the object showed no inflammation, or immunological reaction, by the subject's body to the presence of the object.

The pieces of the object turned black, then red, upon refrigerated storage in blood serum, taken from Mr. Smith. Within 12 hrs of removal, the pieces of the object lined up in the original order, as if trying to re-assemble.

One of the pieces of the object was given to the author of this report for analysis. Mr. Smith stated that after the object was removed, there was a definite, but subtle change in his mood and thought processes, and that he felt more like his "old self".

Analytical Procedure

The sample was inspected with the naked eye, and then imaged under light microscopy, using an Olympus SZ-40 dissecting microscope and an Olympus BH-2 microscope. Magnifications from 10X-400X were utilized.

The sample was then imaged using a JEOL scanning electron microscope (SEM). Magnifications between 150X and >100,000X were utilized. The sample was subjected to energy dispersive X-ray elemental analysis (EDX), along with the SEM imaging.

The sample was then exposed to a strong magnetic field, generated by a neodymium-iron-boron (NIB) magnet, to determine if the sample was magnetic.

Raman laser scattering spectroscopy was also done on the sample, using a Horiba/Jovin Yvon Aramis Raman spectrometer, and 532 nm laser excitation wavelength.

The sample was later (26 November, 2008) sent out to an independent laboratory for more sensitive trace element analysis, using inductively coupled plasma-mass spectrometry (ICP-MS).

Analysis Results

Appearance of Sample

The sample was a small chunk of solid material, approximately cubic in shape, approximately 1 mm X 0.5 mm X 0.5 mm in dimensions, and dark, reddish in color.

The sample was delivered stored in a small, plastic, screw-top medical specimen vial, and covered in blood serum from the patient, to prevent degradation.

Light Microscopy

The sample was first imaged under the dissecting microscope, to obtain low-magnification views (10X-40X magnification) of the entire piece.

Sample in Blood Serum and in Air-10X Magnification

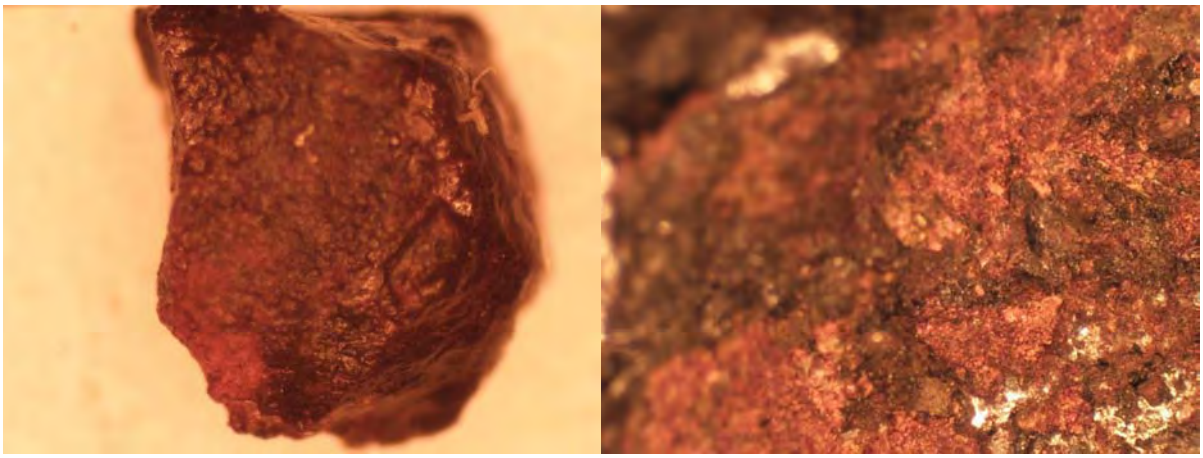

Sample in Air (Left)-and Fragment of Campo Del Cielo Iron-Nickel Meteorite (Right)-Showing similar rusty surfaces

The sample was imaged both in the original container, in blood serum, and in the open air. Drying the sample appeared to cause no degradation.

The low-magnification views of the sample revealed that most of the sample had a somewhat rough, and irregular, surface.

A reddish patina extended over most of the sample surface, which had a color resembling that of iron oxide (rust). The patina also strongly resembled the corrosion product seen on the surfaces of iron-nickel meteorites, which have been exposed to the Earth's atmosphere for some time.

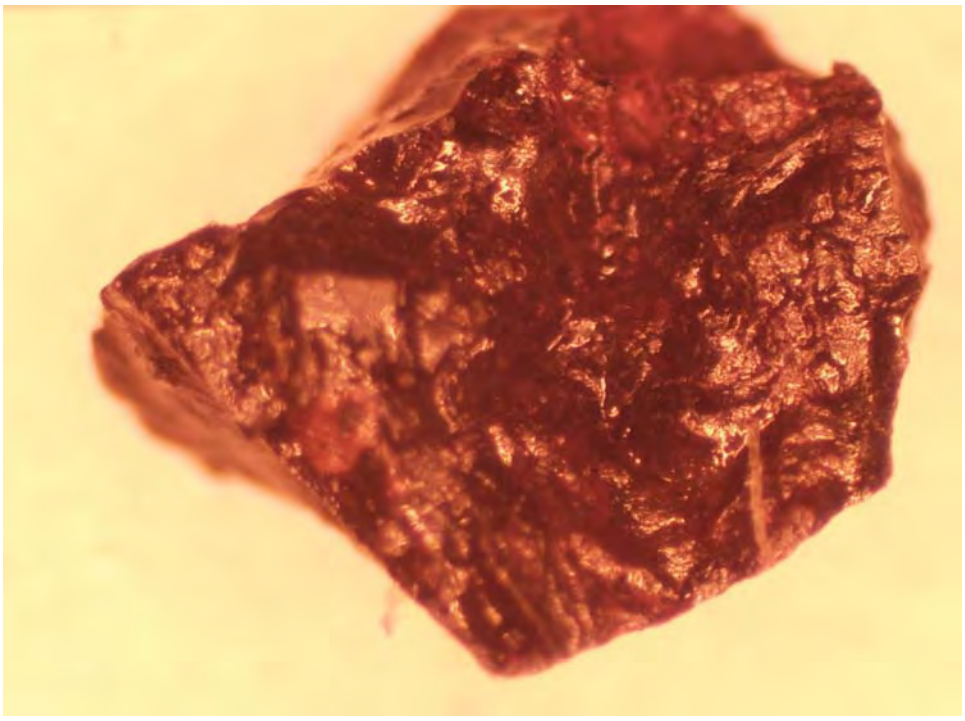

Sample in Air-Showing shiny coating-40X Magnification

A dark, shiny, surface was also observed on the surface of one side of the sample, which remained shiny even after the sample had completely dried.

The sample was then placed under the high-power Olympus microscope, and images taken at 50X-400X magnification.

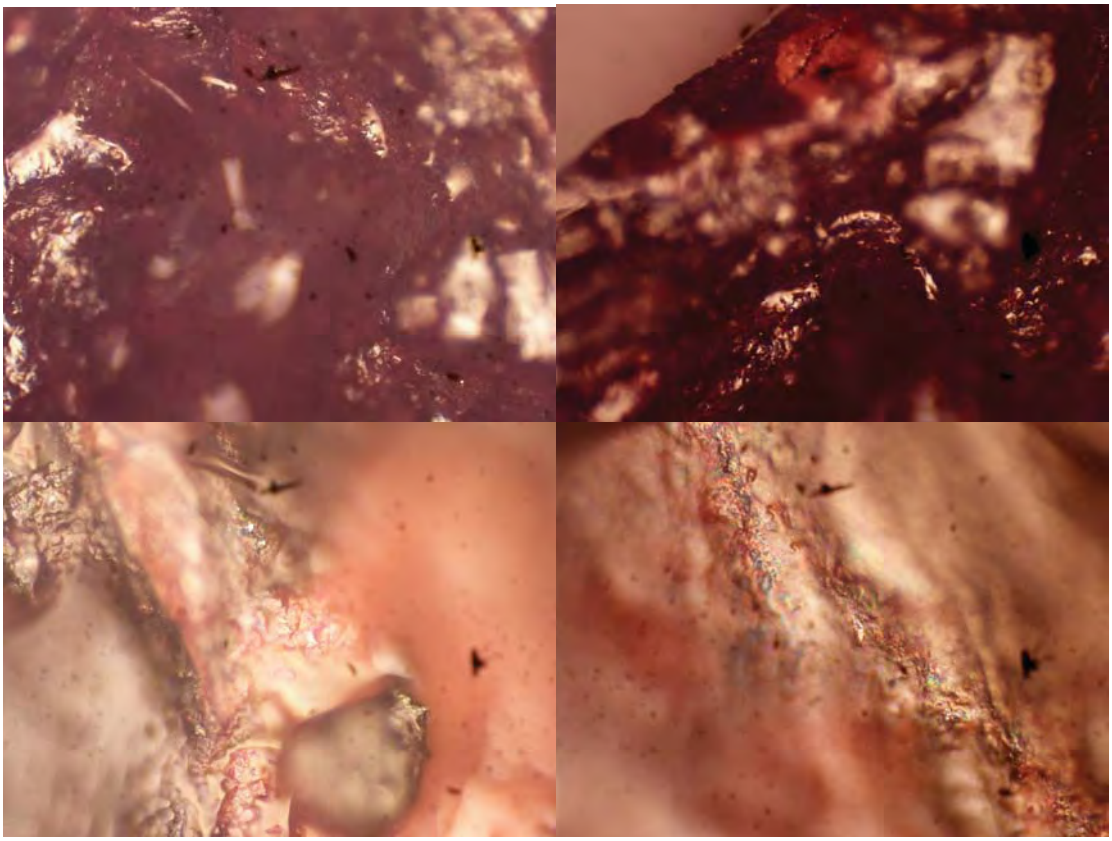

Sample at High Magnification-Showing inclusions of white material and opalescence of shiny surface

Under higher (50X-100X) magnification, inclusions of a light-colored material were evident on the dark, shiny side of the sample.

At 400X magnification, an opalescent sheen was revealed on the shiny material, which resembled that of the mother-of-pearl in abalone shells. Areas of red were interspersed with the areas of shiny, opalescent material.

Scanning Electron Microscopy Imaging

Scanning Electron Microscopy (SEM) imaging was done with gradually increasing magnification, with the first images being taken at a magnification low enough to show any bulk structure possessed by the

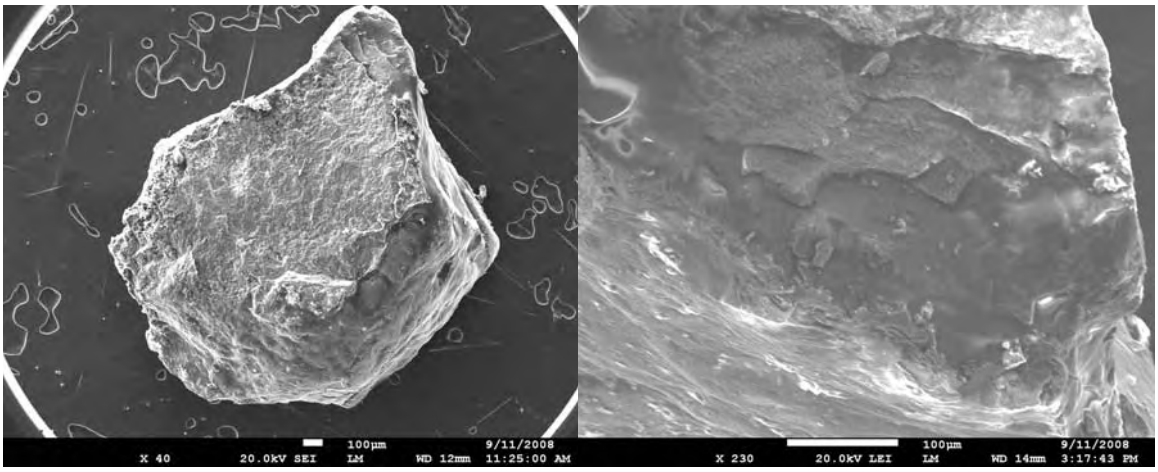

Low magnification Images of Sample (40X and 230X)-Showing whole sample and outer layer over darker bulk material

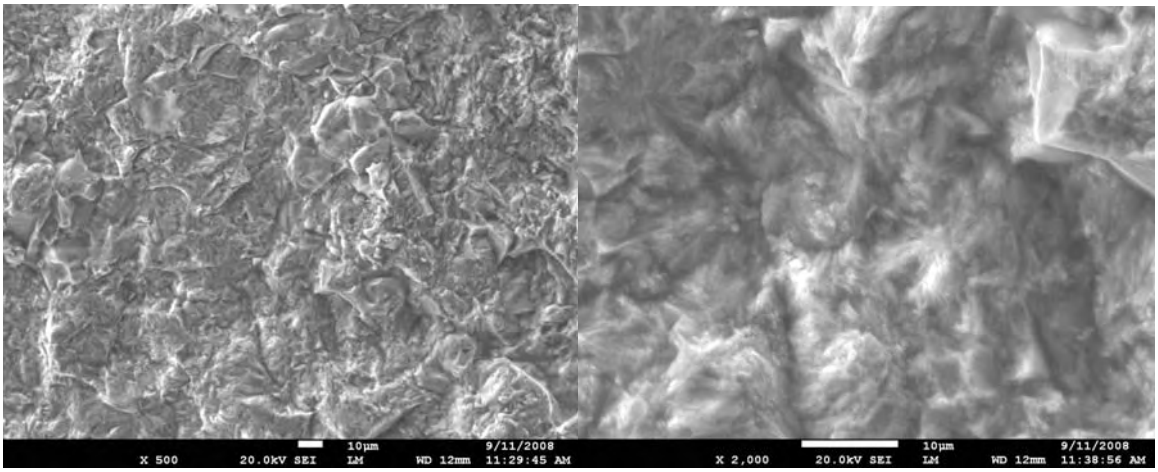

Higher Magnification Views of Shiny Layer of Sample (500X and 2,000X)

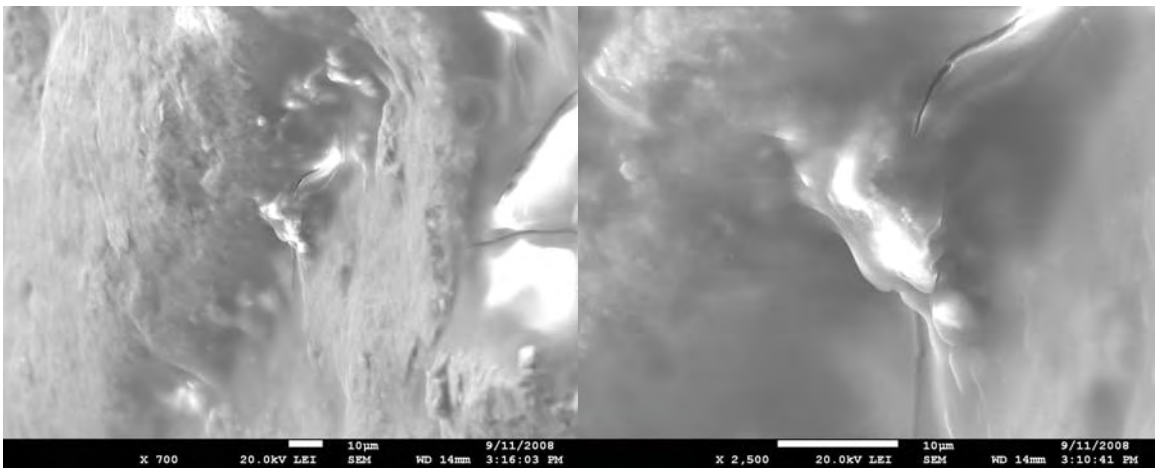

Higher Magnification Views of Dark, Bulk, Portion of Sample (700X and 2,500X)

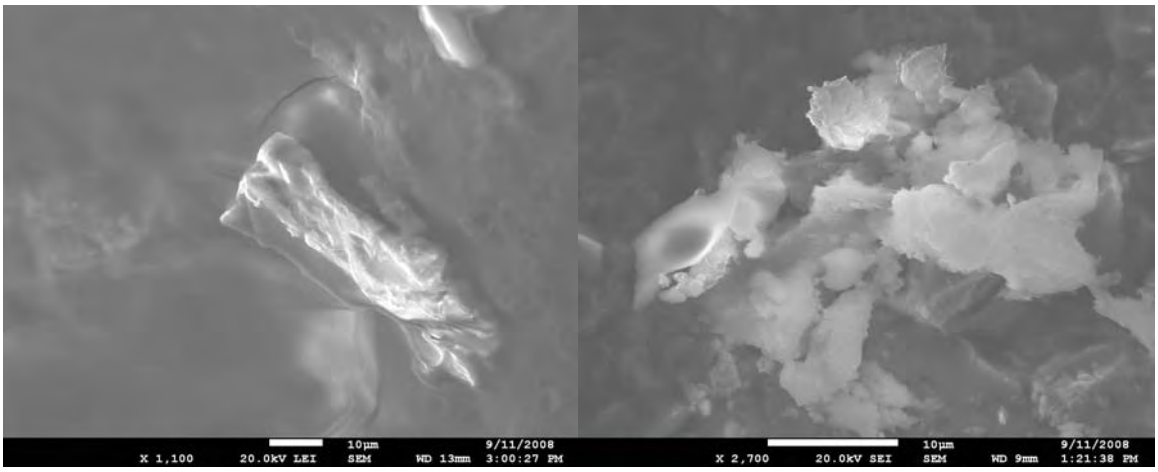

Inclusions of Light Material in Dark, Bulk, Area of Sample (1,100X and 2,700X)

sample. These images showed that the shiny, opalescent, phase seen in the light microscope images appeared to be an outer layer, or coating on the sample. The inner, bulk, portion of the sample consisted of a darker[4] material.

The outer layer of the sample appeared fairly rough, under 500X-2,000X magnification.

The darker, inner, bulk, material of the sample appeared somewhat smoother than the sample outer layer. Some areas of the bulk material appeared quite smooth, with few surface features, other than cracks, and some light-colored areas.

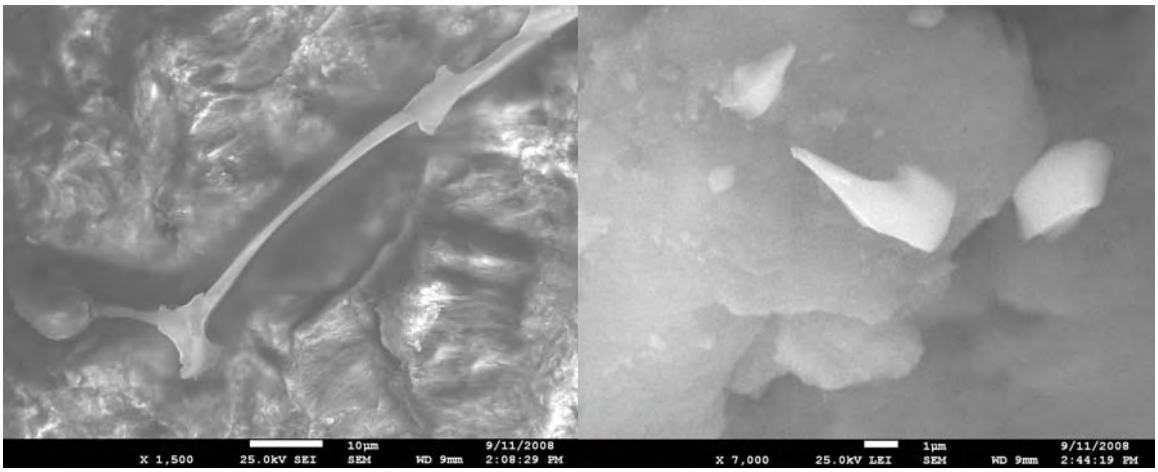

Views of Oddly Shaped Light Material Inclusions (1,500X and 7,000X)

[4] "DARK", IN THE CONTEXT OF SEM IMAGING REFERS TO A SURFACE WHICH ABSORBS ELECTRONS EFFICIENTLY. LIGHT AREAS IN SEM IMAGES ARE THOSE WHICH REFLECT ELECTRONS EFFICIENTLY. IN THIS CASE, THE DARKER MATERIAL, SEEN IN SEM IMAGES, WAS THE FE-NI PHASE (SEE EDX DATA).

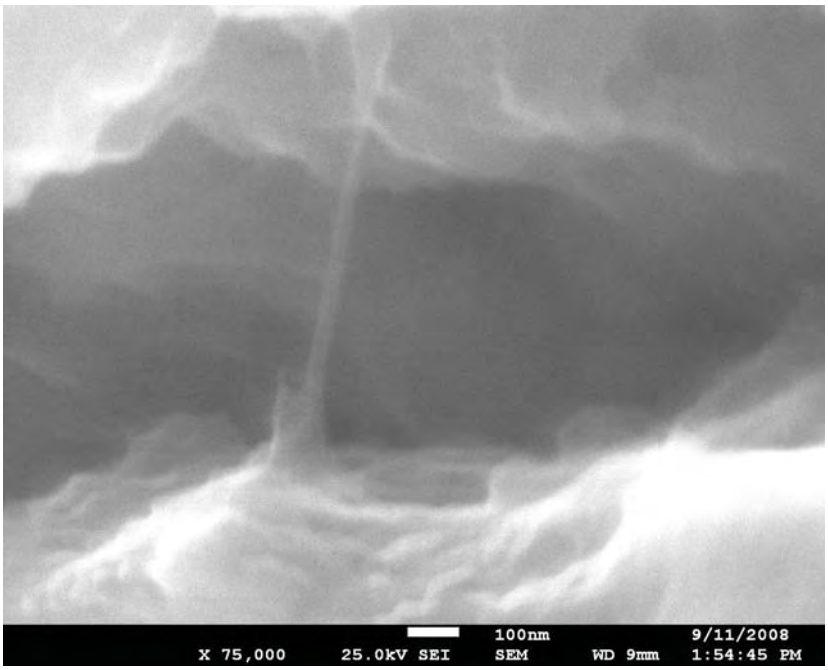

High Magnification Views of Cracks in Shiny Layer of Sample-Showing Nanofibers (75,000X)

Higher magnifications revealed that these light-colored areas resemble the material seen in the outer layer of the sample. Some of these inclusions of the lighter material had unusual, and complex, structures, with sharp, horn-like points, and long bone-like structures.

Nanofibers, approximately 10 nanometers[5] (nm) in diameter, were seen in both the sample outer coating material, and in the inclusions of light material in the dark areas of the sample.

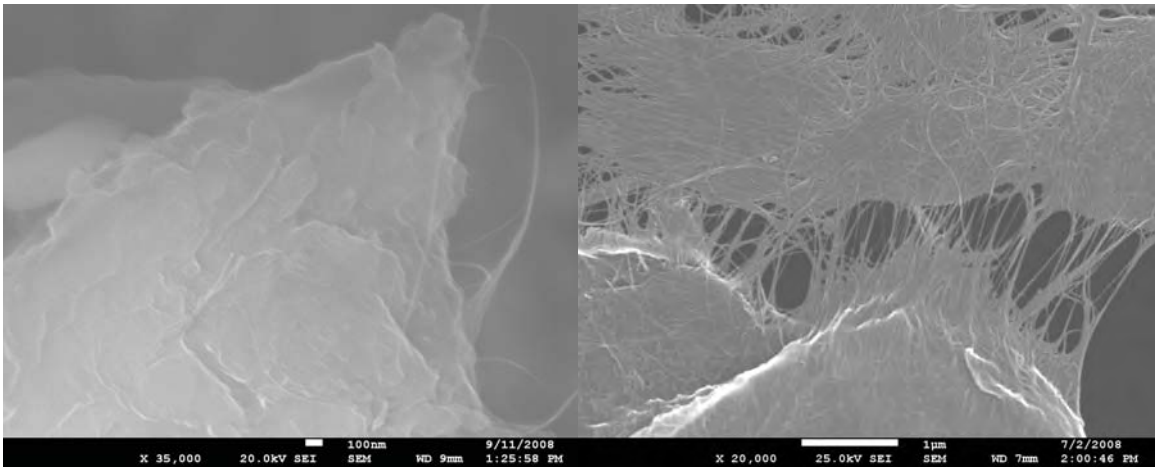

Light Material Inclusion in Dark Area of Sample-Showing Nanofibers (Left, 35,000X) and Carbon Nanotubes (Right, 20,00X)-Shown for Comparison

[5] 1 NM IS EQUAL TO THE WIDTH OF ABOUT 10 ATOMS.

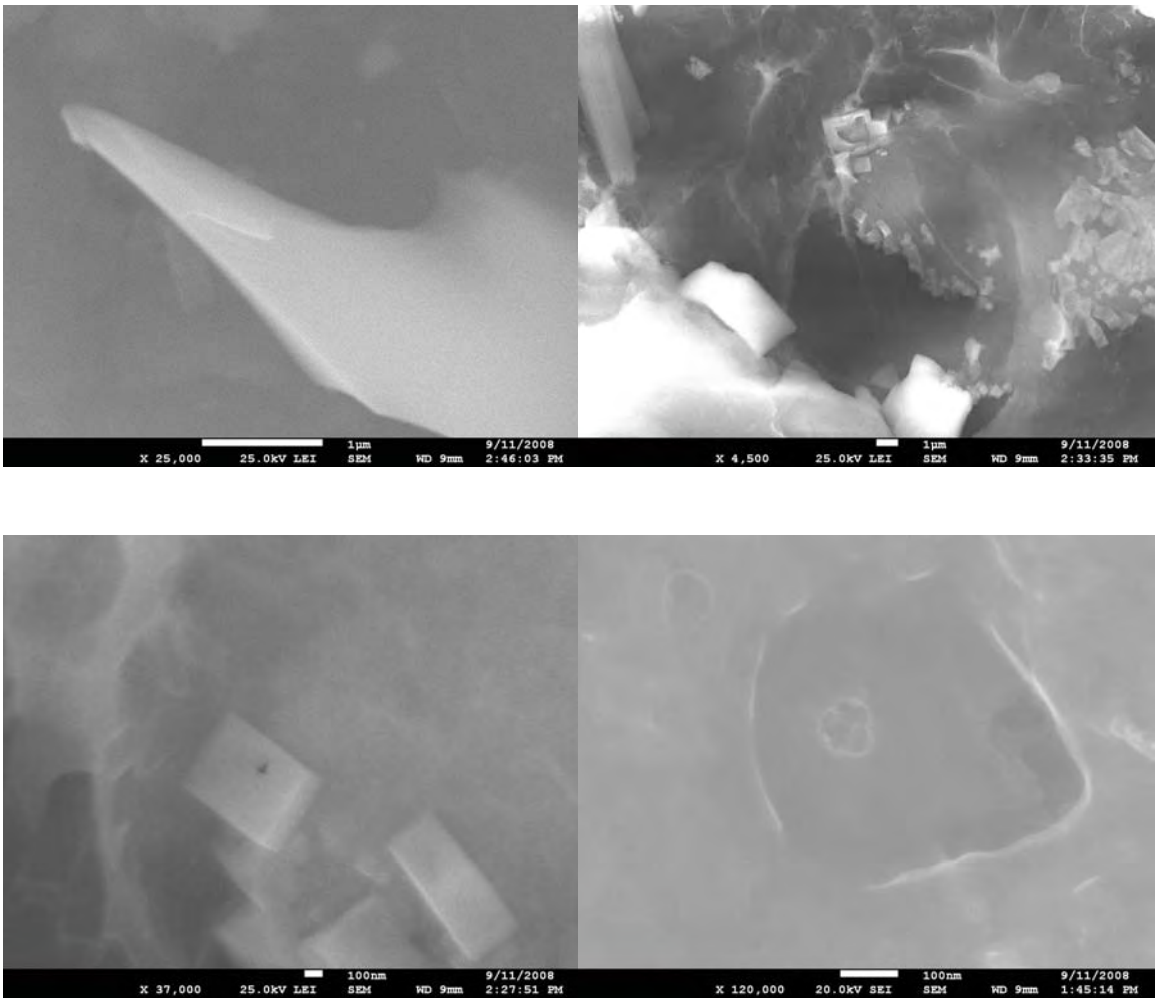

Unusual Surface Structures in Bulk Material of Sample

These nano-fibers resemble bundles of single-walled carbon nanotubes, which are rolled sheets of carbon atoms.

Carbon nanotubes are the strongest known material, and have unique electrical properties. Carbon nanotube research is now one of the leading areas of Materials Science research, and these materials will be used in Earthly science in the future for manufacture of nano-electronic components, ultra-high strength Aerospace materials, and energy storage devices.

Highly regular crystals, and small pits, were also seen in the dark areas of the sample.

EDX Data

Energy Dispersive X-Ray (EDX) scans of a relatively large area of the sample (500X magnification) revealed that the object is composed mainly of oxygen, iron, nickel, carbon, and silicon.

Smaller amounts of magnesium, aluminum, calcium, and sulfur, phosphorus, and sodium also showed up in the initial EDX scans.

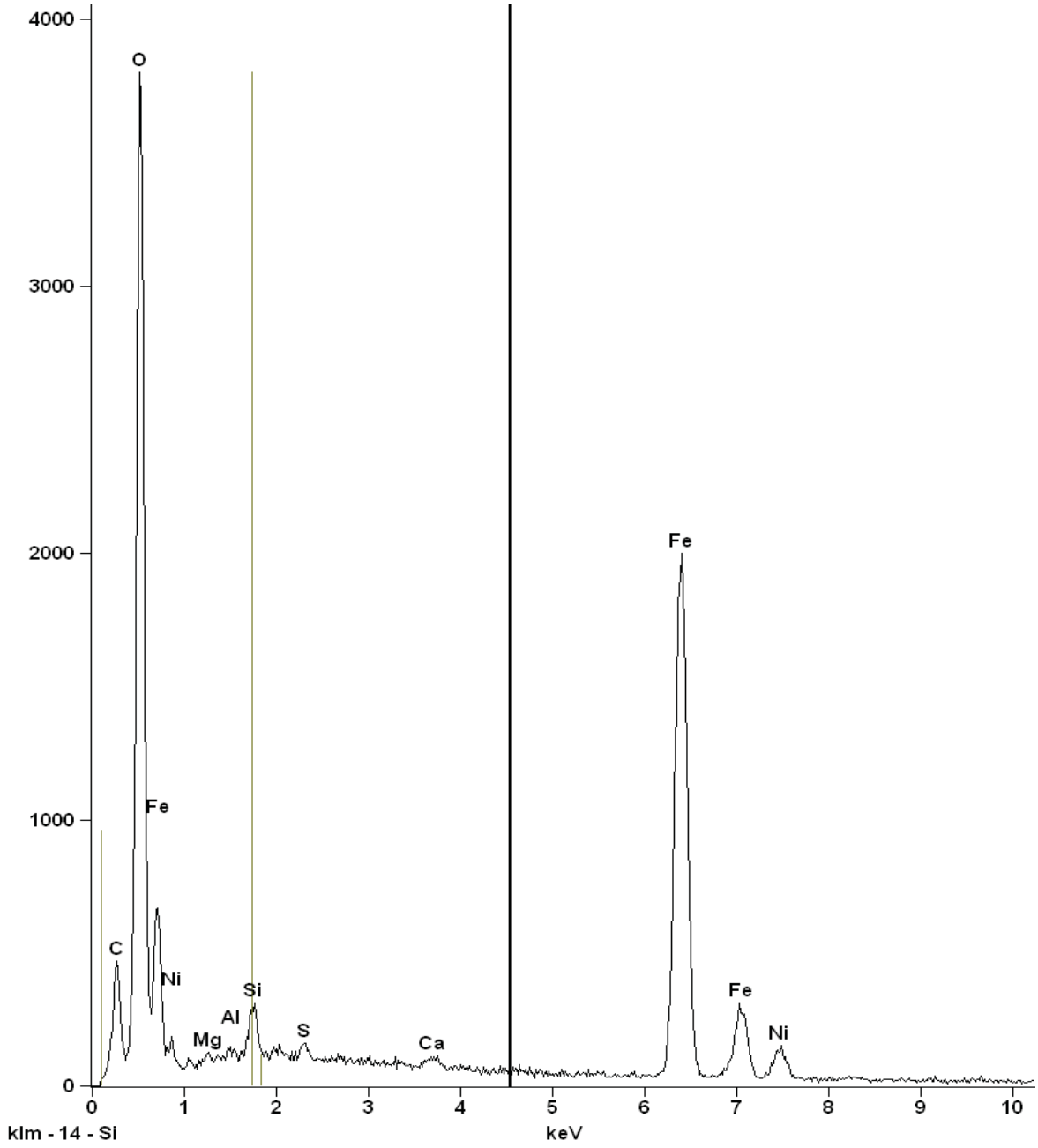

Large-Area EDX Scan of Sample

The small-area EDX scan (point and shoot technique), in which the elemental composition of a very small area in an SEM image is analyzed, was used to determine that the darker areas of the sample are composed mainly of iron and nickel, with a high content of carbon and oxygen, and a smaller amount of phosphorus.

Small amounts of silicon, along with traces of sodium, magnesium, aluminum, phosphorus, sulfur, chlorine, calcium, were also present in the dark material. The EDX instrument software also detected traces of tungsten, and iridium.

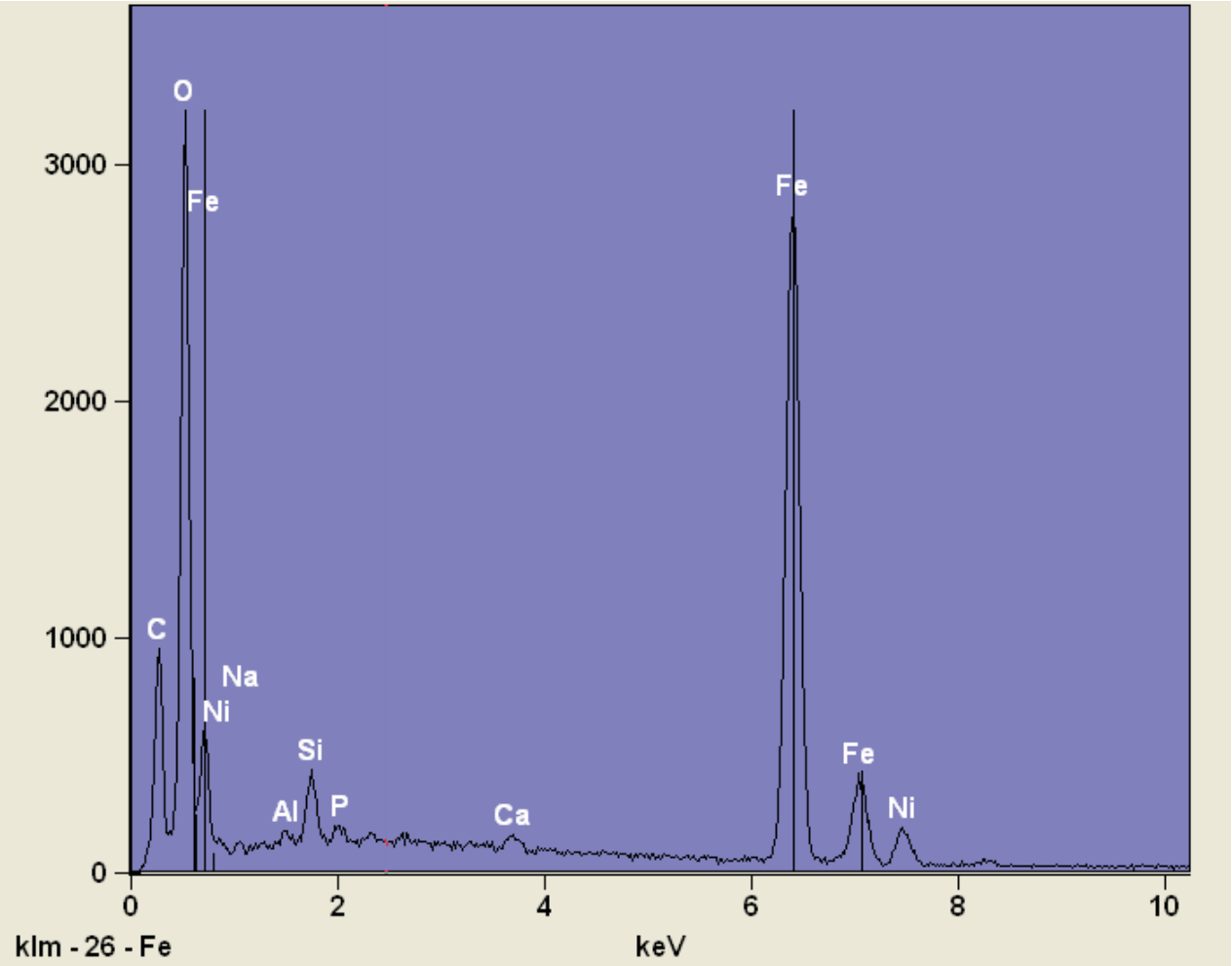

Second Large-Area EDX Scan of Object

The concentration of nickel was found to be 5 wt. %-6 wt. % with respect to the mass of the Fe-Ni sample phase.

The lighter areas of the sample are composed mainly of carbon, oxygen, silicon, sulfur, aluminum, calcium, iron and nickel, with smaller amounts of sodium, magnesium, phosphorus, chlorine, potassium, and titanium , with much lower amounts of iron and nickel.

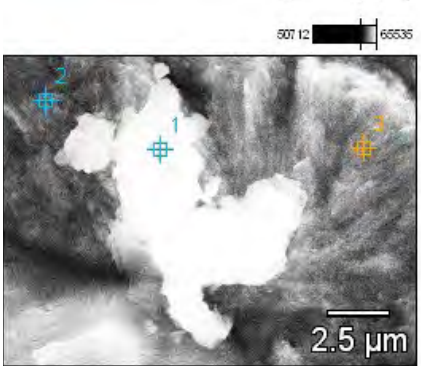

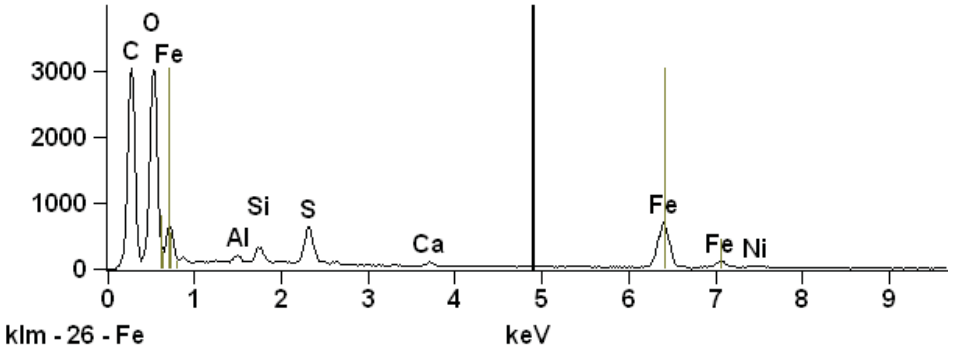

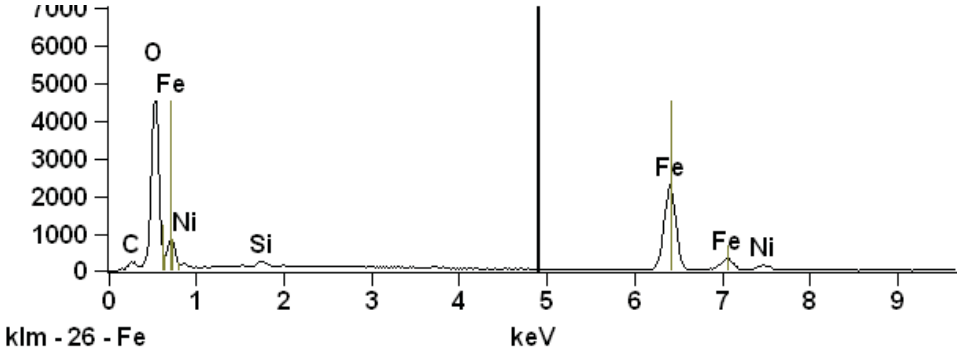

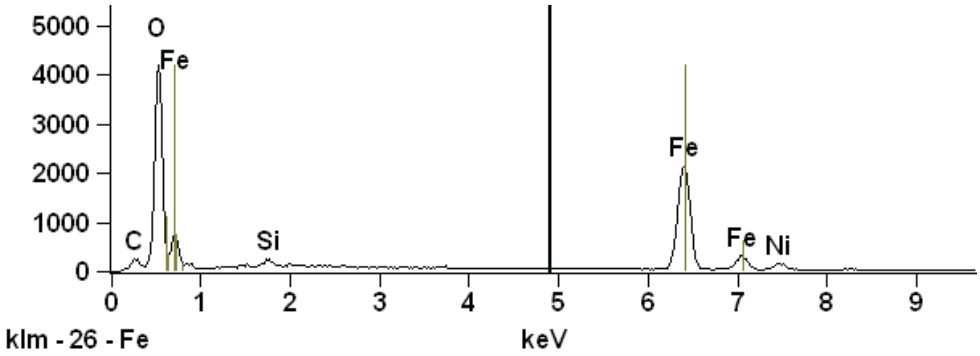

Small Area EDX Scan of Light and Dark Areas of the Sample

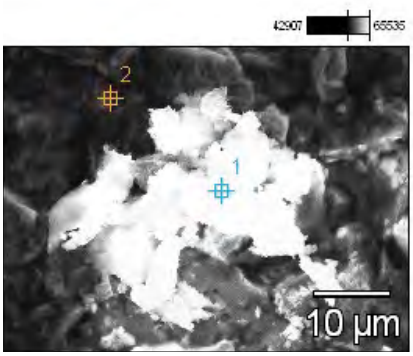

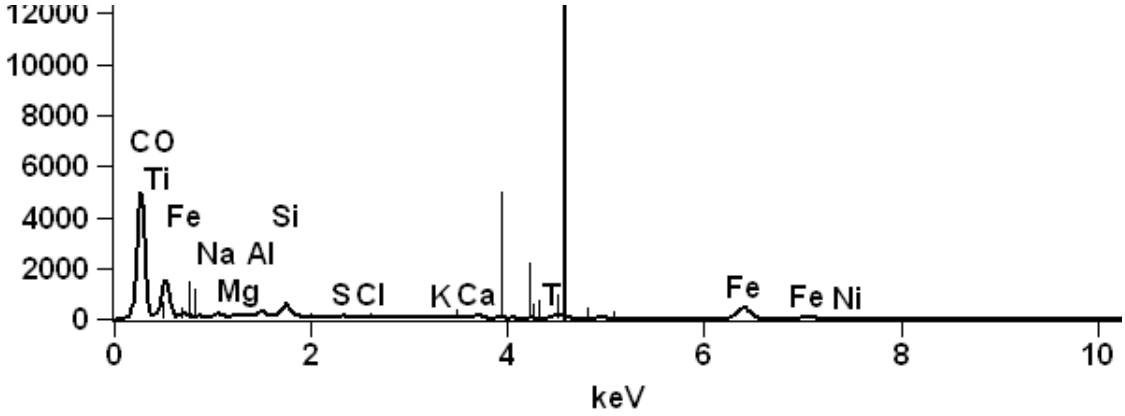

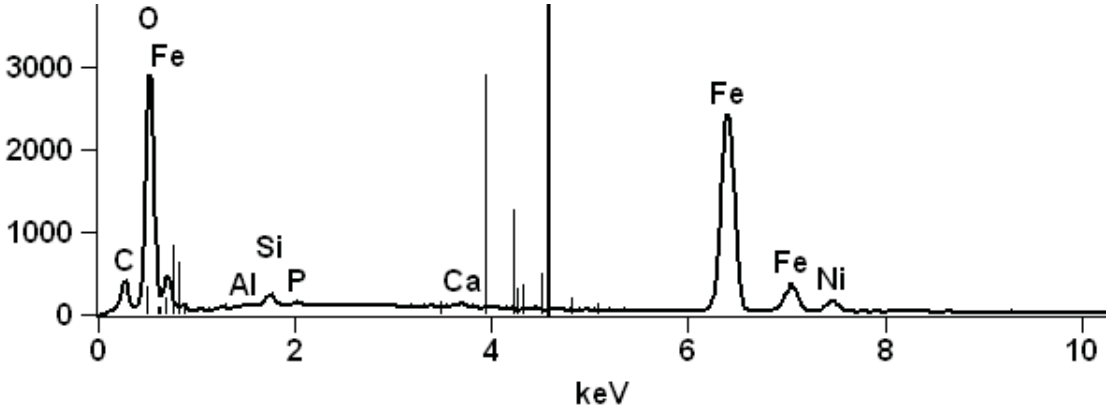

Small Area EDX Scan of Light and Dark Areas of the Sample

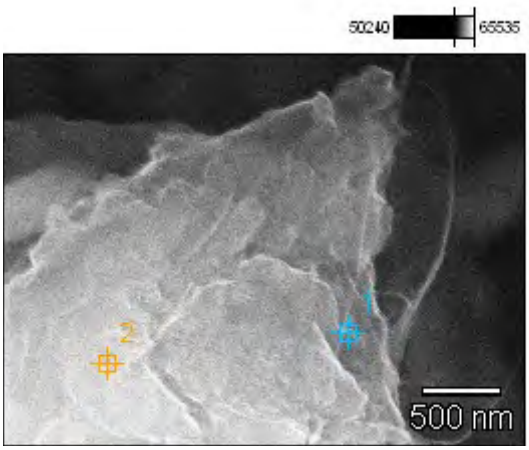

IMAGE NAME: SUN NANO IMPURITY(5)

ACCELERATING VOLTAGE: 20.0 KV

MAGNIFICATION: 35000

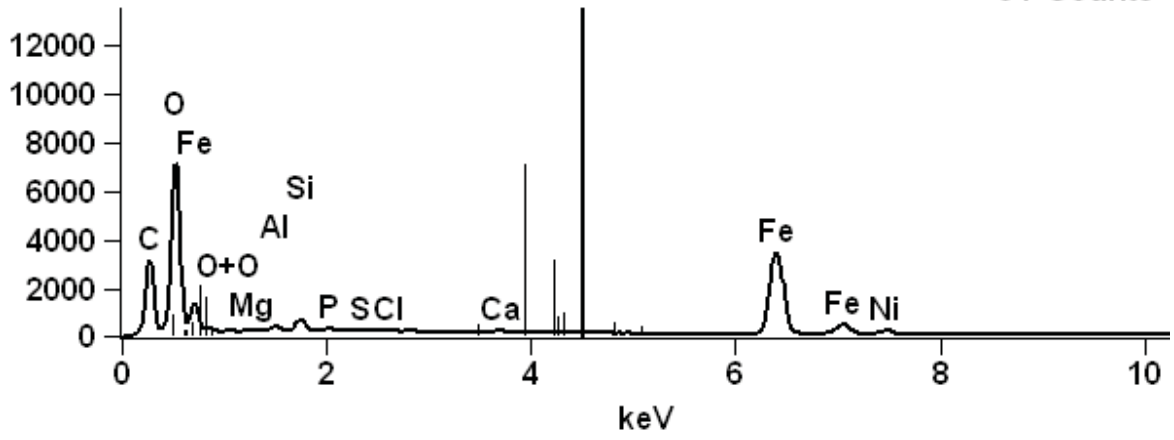

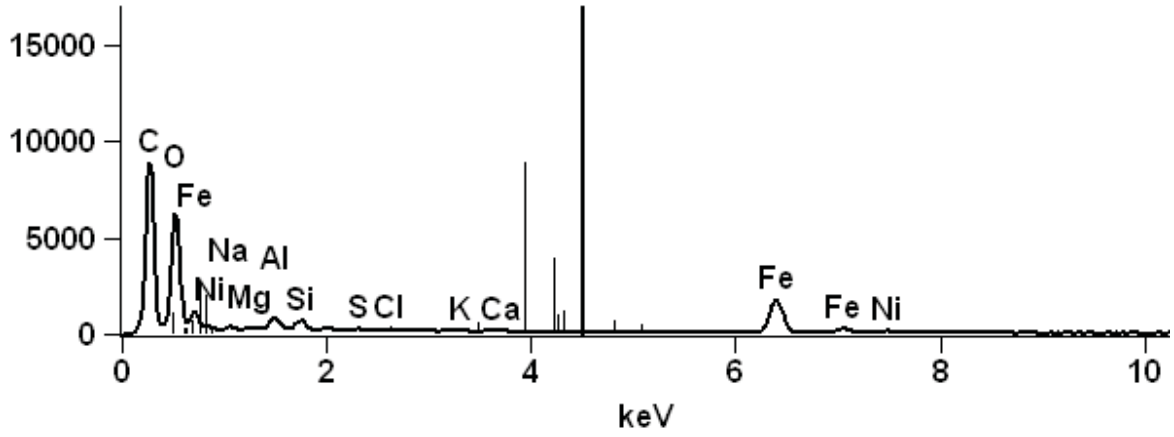

Small Area EDX Scan of Light Area of the Sample-Showing Nanotube Bundles

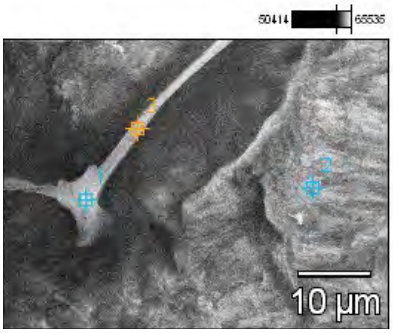

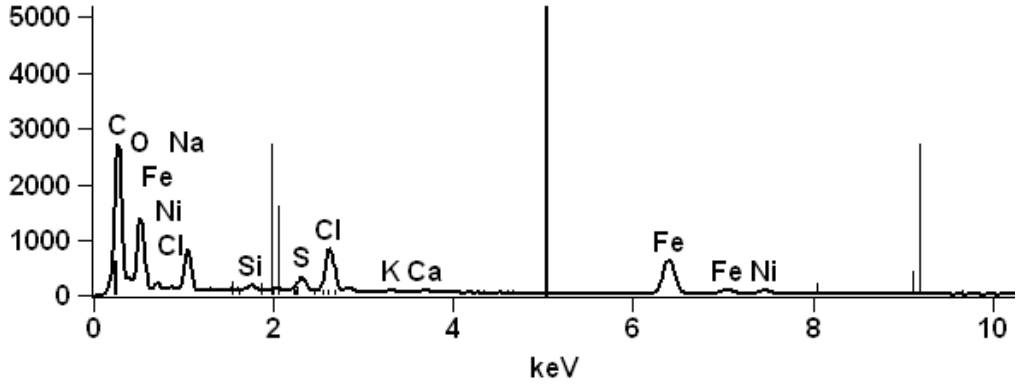

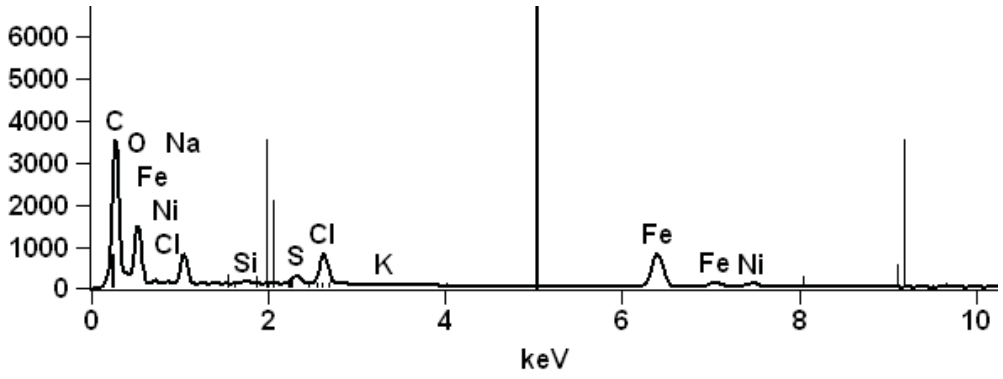

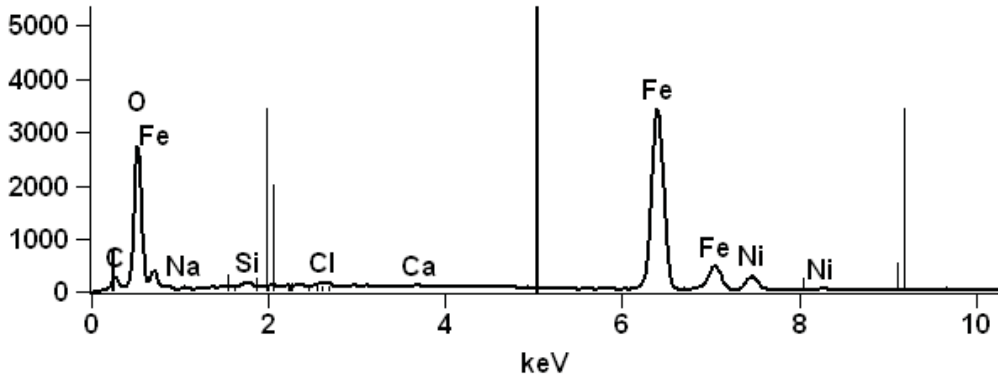

Small Area EDX Scan of Light Area of the Sample-Showing Bone-like Structure

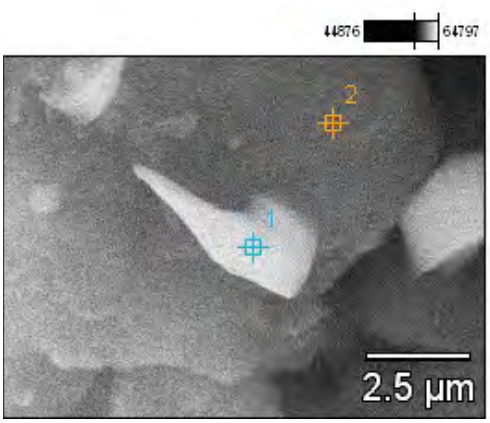

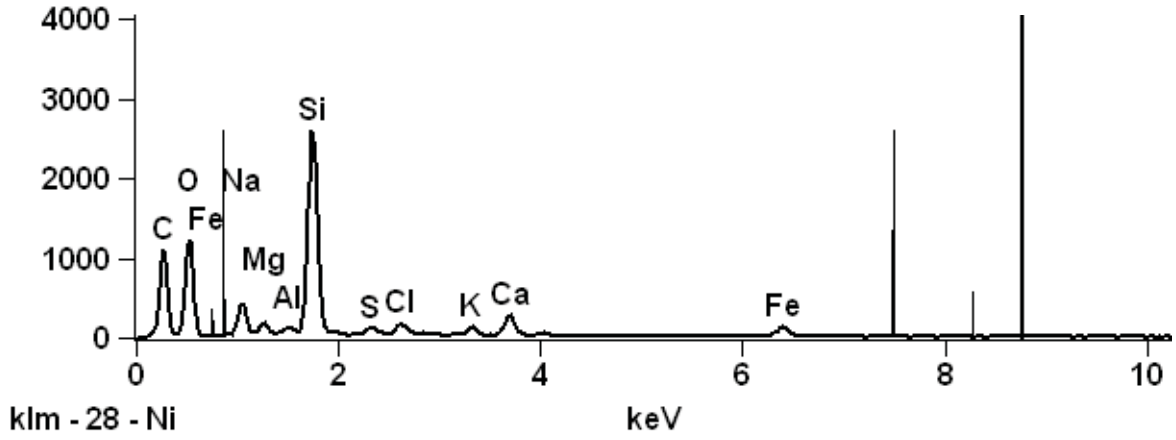

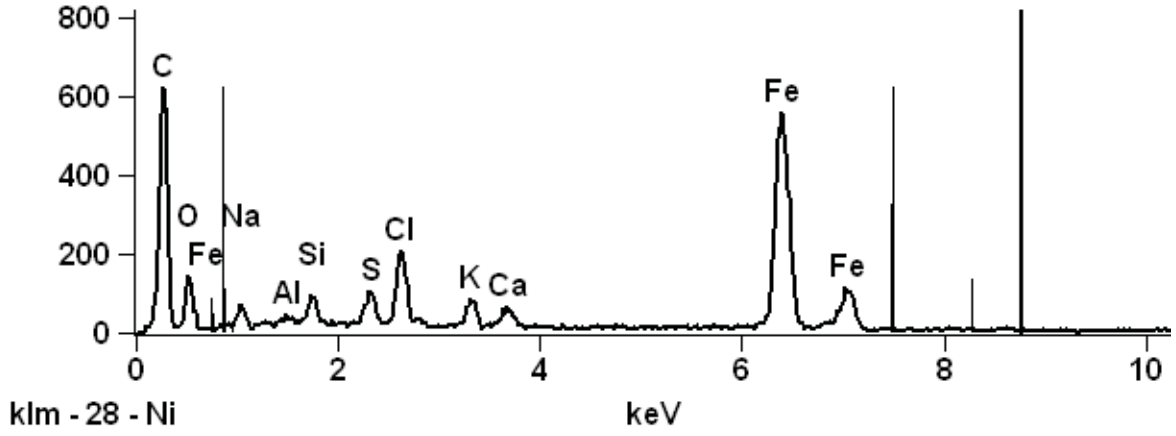

Small Area EDX Scan of Light Area of the Sample-Horn-like Structure-Showing High Silicon Content

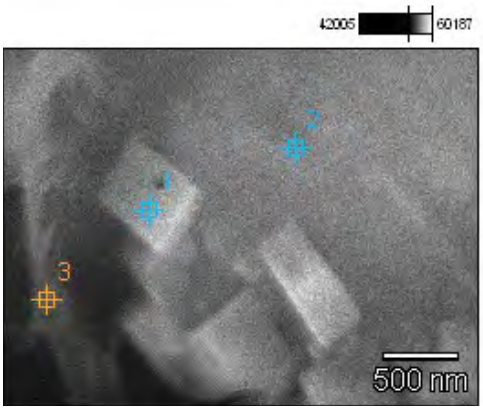
42005
60187
1
2
3
500 nm

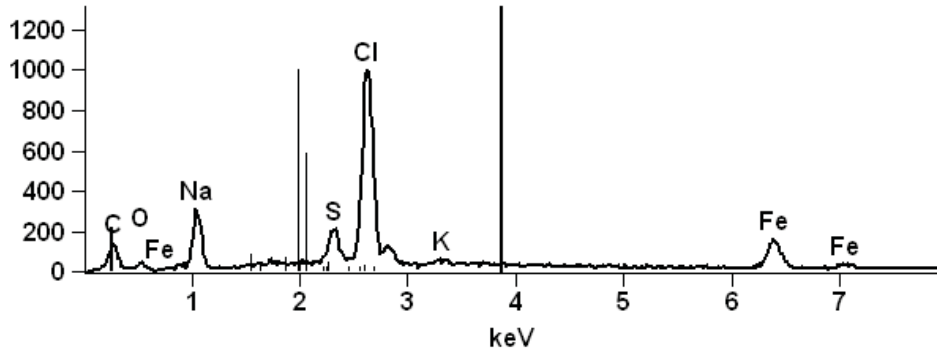
1200
1000
800
600
400
200
0
C
O
Fe
Na
S
Cl
K
Fe
Fe
1
2
3
4
5
6
7
keV

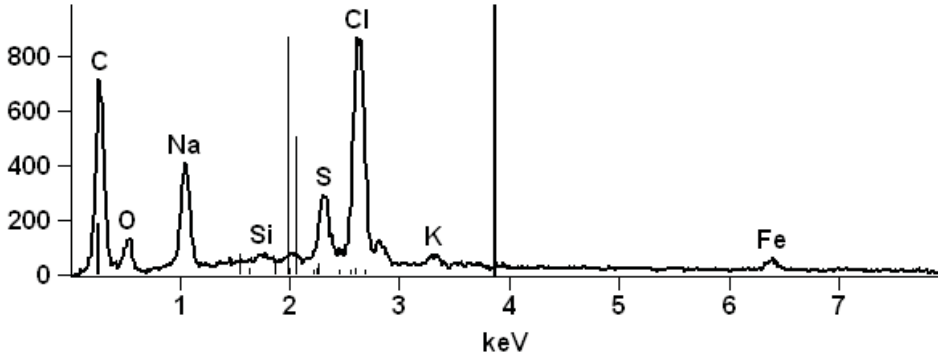
800
600
400
200
0
C
O
Na
Si
S
Cl
K
Fe
1
2
3
4
5
6
7
keV

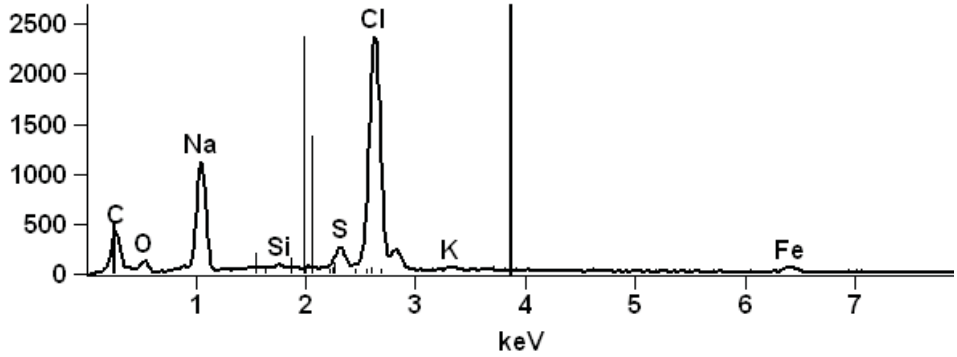
2500
2000
1500
1000
500
0
C
O
Na
Si
S
Cl
K
Fe
1
2
3
4
5
6
7
keV

Small Area EDX Scan of Crystals and Adjacent Areas of Sample

The unusual, horn-like, structures that were seen showed an unusually high concentration of silicon, as compared to the other structures, and areas of light material.

Small (~500 nm) orthorhombic crystals were also imaged, which were mainly composed of sodium and chlorine, with smaller amounts of sulfur, potassium, and iron. It is likely that the metallic elements in the crystals are present as the chlorides, and sulfates. These crystals were distributed in many locations on the dark material of the sample, and were unnaturally uniform in size and shape.

Magnetic Analysis

The sample was found to be strongly attracted to a neodymium-iron-boron (NIB) magnet, and was therefore made of a strongly ferromagnetic material. This is consistent with the presence of large amounts of iron and nickel, as shown by the EDX testing.

Raman Spectroscopy

Raman spectra of the sample were compared to Raman spectra of iron oxide, a sample of iron meteorite, and single-walled carbon nanotubes.

Five of the peaks seen in the low wave-number part of the Raman spectrum of the sample (159 cm^{-1} to 679 cm^{-1}) appear to be a close match to similar peaks seen in the Raman spectrum of the sample of iron-nickel meteorite[6].

The first and last of these four peaks also appear to roughly match two of the peaks seen in the Raman spectrum of the iron oxide sample.

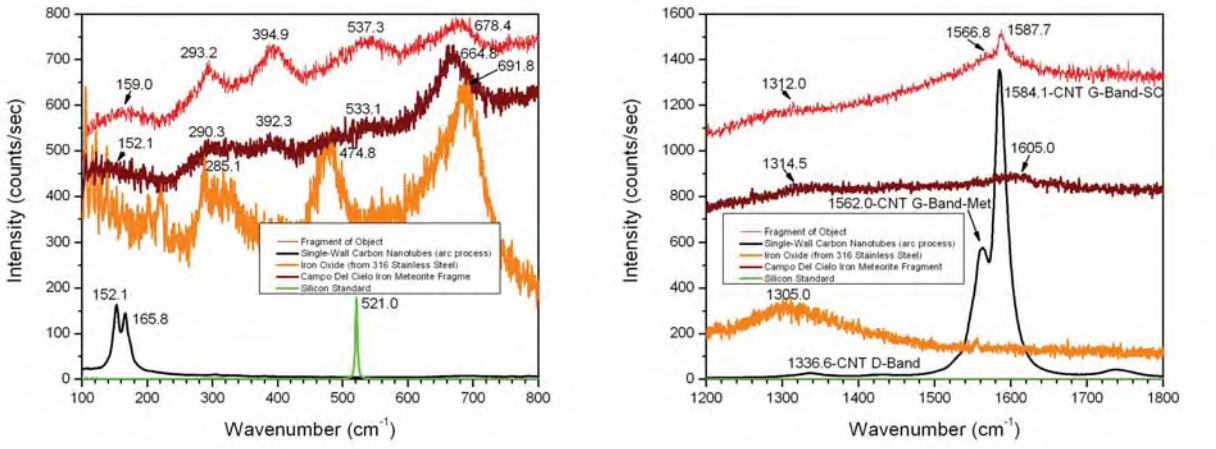

532 nm Raman Spectrum of Sample-as compared to iron oxide, a sample of iron meteorite, and single-walled carbon nanotubes

Three peaks seen in the high wave-number portion of the Raman spectrum of the sample (1312.0 cm^{-1}, 1566.8 cm^{-1}, and 1587.7 cm^{-1}) appear to match the D-band, and both G-band peaks of the Raman spectrum of single-walled carbon nanotubes.

[6] This was a sample of the Campo de Cielo iron meteorite, from Argentina.

Elemental Analysis (ICP-MS)

A more sensitive elemental analysis was performed on a piece of the object removed from Mr. Smith, using inductively-coupled plasma-mass spectroscopy (ICP-MS) analysis, after the SEM, EDX, and Raman data had been obtained. The piece of the sample used was the same one which was analyzed in these previous tests.

The sample piece was digested in a mixture of nitric and hydrochloric acids, and the liquid analyzed by ICP-MS. A portion of the sample, which did not dissolve, proved to contain carbon nanotubes[7].

The ICP-MS elemental analysis confirmed the EDX results, concerning the major components of the sample, and also found many trace elements, which were not detected by EDX. A total of fifty one (51) elements were detected in the sample.

The major components of the sample, in order of abundance, were iron (> 46%)[8], and nickel (5.20%).

Minor component elements, in order of abundance, were silicon (0.27%), cobalt (0.22%), phosphorus (0.16%), and calcium (0.15%).

Major trace elements detected included magnesium (890 ppm, or 0.089%), germanium (300 ppm), aluminum (260 ppm), sodium (230 ppm), copper (170 ppm), and gallium (130 ppm).

Minor trace elements included boron (15 ppm), barium (96 ppm) and strontium (10 ppm), titanium (20 ppm), vanadium (21 ppm), chromium (13 ppm), manganese (62 ppm), zinc (44 ppm), and arsenic (17 ppm).

The sample also contained smaller amounts of precious metals, including platinum (10 ppm), ruthenium (8.0 ppm), iridium (3.6 ppm), palladium (3.3 ppm), rhodium (2.8 ppm), osmium (2.2 ppm), and gold (0.90 ppm).

Other transition elements present included molybdenum (9.3 ppm) and tungsten (1.9 ppm), tin (6.5 ppm), zirconium (4.4 ppm) and hafnium (0.10 ppm), yttrium (0.88 ppm), rhenium (0.66 ppm), and niobium (0.37 ppm).

Elements Detected in Implant Sample by ICP-MS-in Order of Abundance

Element[9]	Amount	Detection	Element	Amount	Detection

[7] This was shown by Raman analysis of the residue; carbon nanotubes are very resistant to the action of most reactive chemicals, and would be expected to survive this type of acid digestion process.

[8] An exact percentage of iron cannot be obtained from this analysis, because the mass spectrometer detector was saturated. The EDX-derived value for the percentage of iron in the sample (~94%) is more accurate, in this case.

	(ppm)	Limit (ppm)		(ppm)	Limit (ppm)
Iron	> 460000	4	Iridium	3.6	0.05
Nickel	52000	0.1	Palladium	3.3	0.02
Silicon	2700	50	Rhodium	2.8	0.02
Cobalt	2200	0.09	Selenium	2.5	1
Phosphorus	1600	10	Osmium	2.2	0.09
Calcium	1500	30	Tungsten	1.9	0.07
Magnesium	890	5	Lead	1.3	0.1
Germanium	300	0.1	Gold	0.90	0.09
Aluminum	260	30	Yttrium	0.88	0.4
Sodium	230	10	Cerium	0.85	0.03
Copper	170	0.3	Rhenium	0.66	0.02
Gallium	130	0.02	Neodymium	0.39	0.02
Barium	96	0.1	Niobium	0.37	0.1
Manganese	62	0.1	Antimony	0.37	0.2
Zinc	44	2	Thorium	0.23	0.02
Vanadium	21	1	Uranium	0.21	0.02
Titanium	20	0.3	Rubidium	0.15	0.02
Arsenic	17	0.4	Samarium	0.13	0.02
Boron	15	3	Gadolinium	0.13	0.02
Chromium	13	0.2	Dysprosium	0.11	0.02
Strontium	10	0.2	Praseodymium	0.11	0.02
Platinum	10	0.02	Hafnium	0.10	0.02
Molybdenum	9.3	0.05	Erbium	0.07	0.02
Ruthenium	8.0	0.02	Ytterbium	0.05	0.02

[9] Red denotes major component elements (100%-1%), green-minor component elements (10,000 ppm-1,000 ppm) blue-major trace elements (1,000 ppm-100 ppm), black-minor trace elements (< 100 ppm).

Tin	6.5	0.1	Europium	0.03	0.02
Zirconium	4.4	0.3			

The sample also contained traces of rare earth elements, and actinides. The rare earth elements detected included cerium (0.85 ppm), neodymium (0.39 ppm), samarium (0.13 ppm), gadolinium (0.13 ppm), dysprosium (0.11 ppm), praseodymium (0.11 ppm), erbium, (0.07 ppm), ytterbium (0.05 ppm), and europium (0.03 ppm). Actinides detected included thorium (0.23 ppm), and uranium (0.21 ppm).

The remaining trace elements detected included selenium (2.5 ppm), lead (1.3 ppm), antimony (0.37 ppm), and rubidium (0.15 ppm).

Potassium was not detected in the ICP-MS analysis, although it was detected in the sample by EDX. It is likely that the amount of potassium in the sample was below the detection limit of the ICP-MS analysis (50 ppm).

Isotopic Analysis

The raw ICP-MS data had sufficient resolution to calculate percentages of isotopes for four of the elements detected in the sample (boron, magnesium, nickel, and copper).

The distribution of isotopes in the elements the sample is made of is a strong indication of the area that the sample was formed. Any deviation of more than 1% of the isotopic ratios in the sample from the terrestrial isotopic distribution indicates that the sample was probably not formed on Earth.

The data showed significant differences between the isotopic distributions of most of the sample elements, for which isotopic data was available, and the isotopic distributions of the same elements obtained from Earthly sources.

The isotopic distributions of the elements in the sample differed by as much as 4% from the terrestrial distributions of the same elements, indicating that the sample probably did not originate on Earth.

Table 3-Isotopic Abundances of Elements Detected in Implant Sample

Isotope	Sample Isotopic Abundance (%)	Terrestrial Isotopic Abundance (%)
B^{10}	17.65	19.9
B^{11}	82.35	80.1

Mg^{24}	75.00	78.99
Mg^{25}	10.97	10.00
Mg^{26}	14.03	11.01
Ni^{58}	67.29	68.08
Ni^{60}	28.24	26.23
Ni^{61}	0	1.14
Ni^{62}	4.47	3.63
Ni^{64}	0	0.93
Cu^{63}	66.80	69.15
Cu^{65}	33.20	30.85

Discussion

The iron/nickel metal matrix which made up the majority of the sample which was analyzed bore a strong resemblance to an iron-nickel meteorite. This is seen by the similarity of the light microscope images of the sample to those of an iron meteorite sample, by the traces of iridium and tungsten seen in the EDX analysis, and by the similarity of the Raman spectrum of the sample to that of a sample of the Campo del Cielo iron-nickel meteorite.

The resemblance of the sample to a meteorite was confirmed by the pattern of trace elements detected in the ICP-MS analysis. The ICP-MS analysis confirmed the presence of traces of iridium, which is very rare on earth, but is universally present in iron-nickel meteorites.

The analysis also showed the presence of relatively large amounts of gallium (130 ppm) and germanium (300 ppm), which are also always present in iron-nickel meteorites, at concentrations in this range.

The presence of traces of precious metals, other than iridium, such as gold (Au), ruthenium (Ru), palladium (Pd), and osmium (Os), are also good indicators of meteoric origin of the metallic portion of the sample.

The elements carbon (C), copper (Cu), cobalt (Co), sulfur (S), phosphorus (P), chromium (Cr), arsenic (As), antimony (Sb), tungsten (W), rhenium (Re), praseodymium (Pr), and manganese (Mn) have also all been detected in iron-nickel meteorites. All of these elements were detected in the ICP-MS analysis of the sample from Mr. Smith's toe.

If the sample matrix material is derived from meteoric iron, its nickel content (5.2%, by ICP-MS, 6% by EDX) is somewhat low, but within the range of nickel percentages published in the literature (5%-25%),

for known iron-nickel meteorites. This concentration of nickel would place the material in a class of low-nickel iron meteorites, known as hexahedrites.

The differences in the isotopic ratios of the sample elements from those which are observed in elements derived from terrestrial sources were quite remarkable, and cannot be easily explained, except by an extraterrestrial origin of the sample material.

Isotopic percentages in elements derived from terrestrial sources have not been observed to vary by more than ±1%, at most, while the variations in the percentages of isotopes observed in the tested sample elements varied by substantially more than this.

The high percentage of iron observed in the chemical analysis data indicates strongly that the red patina on the sample, as delivered, was hydrated iron oxide (rust), a corrosion product formed by contact of the iron in the sample with oxygen, and the water present in the blood serum the sample was stored in. The salts dissolved in the blood serum undoubtedly accelerated the corrosion of the metallic portion of the sample.

The black material, seen on the sample pieces by Dr. Leir, soon after removal from the patient, was freshly formed iron oxide[10], in which hydration had not yet been completed.

The sample had an outer coating of a non-metallic, ceramic-like material, which was approximately 100 nm-200 nm in thickness. This material had a somewhat rough texture, as seen under SEM, with surface irregularities up to several microns in size. Large numbers of inclusions of what appeared to be the same material[11], which were typically several microns in size, were also seen in the metallic phase.

The high concentration of non-metallic, ceramic-like inclusions in the metallic phase probably account for the brittleness of the original object. Inclusions of unlike material, in this size range, which do not bind well with the sample matrix, act as points of stress concentration during episodes of mechanical stress, which leads to cracking at much lower stress levels than would be the case with a homogeneous metallic material.

The presence of these inclusions is the most likely cause of the breakage of the original object into small pieces, during its removal from Mr. Smith's toe.

It is not likely that inclusions of the type observed could have formed within molten iron/nickel, during the formation process of an iron-nickel meteorite, since the solubilities of most salts and ceramics in molten iron is high enough to dissolve a small percentage of inclusions of these materials, especially if these were small in size. It is also difficult to conceive of a natural process in which ceramic inclusions of this type could be formed inside metal, while the metal is in the solid state.

There are, in any event, no known meteorites which contain ceramic inclusions of this type. This is an anomaly, considering the fact that all the other evidence appears to point to a meteoric origin for the sample.

---

[10] THIS MATERIAL (Fe_2O_3) IS BLACK IN COLOR, AND TURNS RED AFTER LONG EXPOSURE TO WATER.

[11] EDX ELEMENTAL ANALYSES OF THE INCLUSIONS AND THE OUTER COATING WERE VERY SIMILAR.

The non-metallic, ceramic-like, material contains mainly carbon (C), oxygen (O), silicon (Si), sulfur (S), aluminum (Al), calcium (Ca), iron (Fe) and nickel (Ni), with smaller amounts of sodium (Na), phosphorus (P), chlorine (Cl), potassium (K), and titanium (Ti), and chemically resembles a biological hard part, such as shell, or bone.

This similarity of the composition of the non-metallic phase to biological material may be partly responsible for the lack of immune response to the object by the patient's body.

The opalescence of this material, seen in the light microscopy images, indicates the presence of an organized, layered, structure, such as occurs in mother-of-pearl, or opal, which reflects and refracts light strongly into different color bands.

The Raman data, showing what appears to be carbon nanotube D-Band and G-Band signals strongly indicates the presence of carbon nanotubes (CNTs). This is confirmed by the SEM images, which show bundles of nanotubes, with high carbon content (EDX data), which appear nearly identical to SEM images of commercially produced, arc-process, single-walled CNTs. Carbon nanotubes have never been found in naturally occurring materials, to date.

The data therefore indicates that the majority of the non-metallic phase material is probably composed mainly of carbon nanotubes, which are covered, and/or filled, by a shell-like coating of aluminum, calcium, iron, nickel, and titanium silicates, oxides, sulfates, and phosphates.

The shapes of the inclusions of the lighter, non-metallic, material in the Fe/Ni phase appear to be non-random, such as the long bone-like, and horn-like structures seen in the SEM images. The Fe/Ni phase also has numerous pits, of regular size (400 nm-500 nm) and shape.

The carbon nanotubes inside the structures would be excellent carriers of electric current, and could also act as electronic components. The shell-like coating on the material would provide good electrical insulation for these nano-components.

The relatively large amounts of silicon and germanium in the sample may also indicate the presence of silicon-based, and/or germanium-based electronic components in the sample.

A smaller percentage of the non-metallic phase of the sample is composed of the very regularly sized (500 nm), and shaped, sodium, potassium, and iron, chloride and sulfate-containing crystals, seen in the SEM images.

These crystals appear to be far too regular in size and shape to have formed spontaneously, from drying of the salts in the blood serum the samples was stored in. Crystal like this could have acted as resonators[12] for generating the radio signals which the object was emitting before it was removed.

Because the ceramic/carbon nanotube inclusions and crystals appear to be artificially shaped nano-components, the carbon nanotubes in the inclusions are not found in nature, and the fact that the complete object was giving off radio signals, before removal, the conclusion is inescapable that the object the sample came from is a manufactured device, which was inserted in Mr. Smith for a definite purpose. This

[12] CRYSTALS, SUCH AS QUARTZ CRYSTALS, HAVE BEEN USED FOR MANY YEARS TO GENERATE VERY PRECISE RADIO FREQUENCIES.

device was apparently made using extraterrestrial materials, by an organization possessing a high degree of technological sophistication.

The differently shaped inclusions of the non-metallic, CNT-containing material could be for the performance of different functions in the device, such as carrying electric current (bone-like structures), acting as antenna for emitting, or receiving, radio signals (horn-like structures), or acting as resonators, to generate the radio waves (salt-containing crystals).

The magnetic nature of the metallic matrix material of the object may be necessary for the device, to function, or, alternatively, meteoric iron could have been chosen as a base material simply because of its abundance in our solar system, and probably other solar systems, as well.

This would make it a relatively inexpensive metallic material for use in manufacture, if the organization, or society, that made the object already had inexpensive methods of space transport, and travel.

The manufacture of a device comparable to this one is probably beyond the technology of known, Earthly, commercial processes, at the present time. It is most likely, therefore, that the device was manufactured by an alien civilization.

The function of the device cannot be determined with certainty from the available data, and the device may have had multiple functions and missions. Because the device was connected to Mr. Smith's nervous system, it is likely, however, that two of its functions had to do with monitoring of the physiological state of Mr. Smith's body, and mood/mind control.

Bibliography

Lithium Isotope Analysis of Inorganic Constituents of the Murchison Meteorite-Mark A. Sephton, et. al.; The Astrophysical Journal, 612:588-591, September 1, 2004

Boron Isotope Ratios in Meteorites and Lunar Rocks-Zhai, et. al., Geochimica et Cosmochimica Acta, vol. 60, Issue 23, 12/1996, pp.4877-4881

Carbon Isotope Abundance in Meteoritic Carbonates-Robert N. Clayton; Science, 12 April (1963) pp. 192-193

Ti^{50} Anomalies in Primitive and Differentiated Meteorites-Goldschmidt Conference Abstracts, A1038 (2007)

Measurements of the Isotopic Ratios of Nickel in Iron Meteorities, Using Nickel Carbonyl-Masaru Suzuki and Sadao Matsuo; Geochemical Journal, vol. 1, pp. 50-60, 1967

Nickel Isotope Anomalies in Meteorites and the Fe^{60}-Ni^{60} Clock-M. Bizzarro, et. al.; Workshop on Chronology of Meteorites (2007)

Germanium Isotopic Fractionation in Iron Meteorites-64th Annual Meteoritical Society Meeting (2001)

Tungsten Isotope Evidence from 3.8-Gyr Metamorphosed Sediments for Early Meteorite Bombardment of the Earth-Shoenberg, et. al.; Nature 418, 403-405 (25 July 2002)

Tungsten Isotopic Constraints on the Formation and Evolution of Iron Meteorite Parent Bodies-A. Markowski, et. al.; Dept. of Earth Sciences, Oxford Univ.; Lunar and Planetary Science XXXVI (2005)

Microanalysis of Platinum Group Elements in Iron Meteorites Using Laser Ablation ICP-MS- A. J. Campbell and M. Humayun, Dept. of Geophysical Sciences, Univ. of Chicago;

Lunar and Planetary Science XXX (1974)

New Applications of the Re187-Os187 and Pt190-Os186 Systems to the Study of Iron Meteorites-D. L. Cook, et. al., Isotope Geochemistry Laboratory, Dept. of Geology, Univ. of Maryland; Lunar and Planetary Science XXXI

Compilation of Minimum and Maximum Isotope Ratios of Selected Elements in Naturally Occurring Terrestrial Materials and Reagents-Coplen, et. al.; U.S. GEOLOGICAL SURVEY Water Resources Investigation Report 01-4222

Meteorites: A Petrologic, Chemical and Isotopic Synthesis-Cambridge Planetary Science Series-R. Hutchinson; Cambridge University Press (2004)